Microclimate monitoring for smart agriculture

T.J. Bieling (4399803), A.A. Koekkoek (4475291), S.J.M. van der Maarel (4443314), J.A. Ravenhorst (4491319)
The Department of Precision and Microsystems Engineering, BEP Group A4

***Abstract*— An ultrasound based temperature measurement and mapping method is described. Three different methods of determining the time of flight are proposed. Using a function generator and an oscilloscope, the temperature was determined over a fixed distance. A clear difference in time of flight between a heated and unheated line was measured leading to a clearly distinguishable temperature. Mapping of the temperature is possible with the help of the SIRT method described in the paper. With the results and recommendations from this paper, a spatial mapping of temperature distribution can be obtained.**

I. Introduction

An increasing world population, climate change, pollution and urbanization force agriculture to produce more efficiently and sustainably. Solutions might tend towards high tech solutions such as closely monitoring the environment of crops on a small scale, using sensor technology. Temperature mapping in greenhouses could be part of that. A conventional method such as in-field sensor nodes can be used for temperature mapping. Contrary to in-field sensor nodes, ultrasound time of flight measurements could provide an off-field means of mapping temperature. This leads to the following research question: How do ultrasound time of flight measurements compare to sensor nodes for determining spatial temperature distributions?

For sensor nodes and ultrasound, a test setup around a 2 by 2 meter field will be built in combination with algorithms to make a spatial temperature mapping.

In an article by A. Raabe et al. [1], acoustic tomography in a 200 by 260 meter field provides a temperature mapping. That is done with 1000 Hz sound instead of ultrasound, but it does show the viability of the concept. In an article by Mizutani et al. [2] successful mapping of temperature using ultrasound was reported on a 0.1 by 0.1 meter field. Scientists at the Tokyo Institute of Technology were able to map the temperature on a 1 meter diameter circle, according to an article by Ohyama et al. [3]. The researches mentioned, apart from the first research, use a smaller field than in this research. In addition, all three researches do not clearly substantiate the algorithms used to retrieve a temperature distribution.

This research is conducted as part of the Bachelor End Project of Mechanical Engineering at the TU Delft. It was done as a research study for the Plantenna project.

II. Theory

By using the time of flight of an ultrasound signal between a sender and receiver, the speed of sound can be calculated for a fixed distance:

$$c = \frac{x}{t} \tag{1}$$

With x the distance in meters and t the time in seconds. The wind speed is neglected for this research. Rewriting the temperature as a function of the speed of sound in dry air, from Aldawi et al. [4], gives equation 2 with T in °C and c in m/s:

$$T = ((\frac{c}{331.3})^2 - 1) \cdot 273.15 \tag{2}$$

For more information mail t.j.bieling@student.tudelft.nl

III. Methods

A. Sensor nodes

To get an idea of temperature distribution in a closed room, 16 STEVAL-SMARTAG1 sensor nodes were placed in a field of 2 by 2 meters with equal distances in between. These nodes measure the temperature at given time steps. An algorithm was developed to create a temperature mapping by interpolating between the temperatures given at the locations of the nodes. This method will later on be used to validate the ultrasound mapping algorithms.

B. Ultrasound

In this research, piezoelectric ultrasound transducers that oscillate at 40 kHz are used. These transducers convert oscillations into an electric charge and vice versa. To accomplish the measurement of the time of flight itself, a one dimensional test setup was designed which is depicted schematically in figure 1.

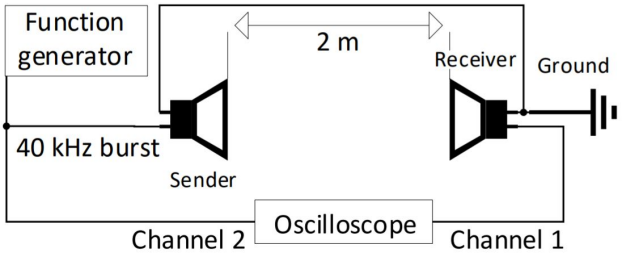

Fig. 1. The one dimensional test setup

An eight cycle, 20 V peak-to-peak, 40 kHz burst from a function generator excites the sender that emits a 40 kHz signal, which is received 2.00 meters away. An oscilloscope processes the electrical signal of both the sender and the receiver using an averaging function: The waveform resulting from one measurement is a result of averaging 256 sub-measurements.

C. Experiment

An experiment was carried out to verify how well the system and algorithm works with a 2.00 meter line average with and without a heater to change the temperature.

No heater was used for the first 25 measurements. The temperature between the sender and receiver was constant at 21.9 ± 0.5 °C, according to a BK Precision Model 625 hand-held thermometer.

The next set of 25 measurements was done using a heater. The heater was put underneath, and parallel to the direct path of ultrasound bursts. The heater covered 28 ± 2 cm of the 2.00 meter path. The temperature above the heater fluctuated strongly according to the hand-held thermometer; 41 ± 3 °C. The rest of the line segment had a temperature of 24 ± 1 °C. Due to the availability of only one hand-held thermometer, and the turbulent nature of the air flows near the heater, it is hard to estimate the line average. Very roughly assuming a constant temperature directly above the heater, and a constant temperature in the rest of the path, would imply a line average temperature of 26 ± 1 °C.

D. Signal processing

Per measurement, and per sender and receiver, the data obtained consists of 45000 samples of the time and voltage of the signal. A digital band-pass filter is used to remove the noise. The equation for the time of flight can be written as:

$$ToF = t_{receive} - t_{send} \tag{3}$$

With t_{send} the time of the first local maximum of the 40kHz sending signal (the blue signal in figure 3). $t_{receive}$, the time when the signal arrives at the receiver, is determined in three different ways. The received peak between 0 and 1 ms (figure 3) is assumed to be an echo of a previous burst. It does not influence the measurement.

Method 1: $t_{receive}$ is calculated as the time point of the peak (local maximum of the absolute signal) where the voltage of the received signal is 95% or higher than the peak directly right of it. This is an iterating process for finding the first peak left of the highest point of the received signal that meets the following condition:

$$y(t_n) > 0.95 \cdot y(t_{n+1}) \tag{4}$$

with $y(t)$ for all local maxima.

Methods 2 and 3: The envelope of the received signal is extracted and its maximum is determined. Then an iterative process finds the first point in the slope, where the derivative is smaller than an empirically determined value that distinguishes the signal from the noise. From this point, method 2 uses a linear approximation to zero to determine $t_{receive}$. Method 3 uses an exponential approximation to zero in order to determine $t_{receive}$.

E. Setup

To test the temperature mapping, eight pairs of MA40S4S and MA40S4R sensors, both from Murata, were installed in a setup that is schematically drawn in figure 2. The black blocks represent senders, the grey blocks represent receivers. They lead to 48 possible line measurements because each sender can reach six receivers.

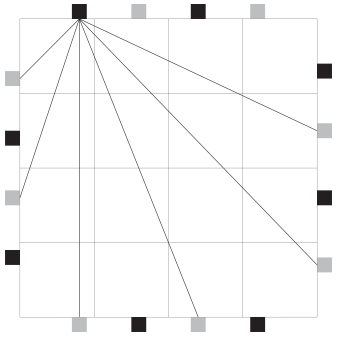

Fig. 2. The two dimensional test setup

F. SIRT and pseudoinverse

The output of the ultrasound temperature measurement system is a set of times of flight, which gives mean times of flight along the lines between ultrasound transducers. If the field over which the temperature is measured is divided into a square grid field of n tiles, then the mean time of flight given by the ultrasound lines are given by the following equation:

$$ToF_{mean} = r_1 \cdot ToF_1 + r_2 \cdot ToF_2 + ... + r_n \cdot ToF_n \tag{5}$$

Where ToF_n is the mean time of flight across the n^{th} tile and r_n is the ratio of the total length of the ultrasound line that crosses the n^{th} tile. Let A be an $n \times m$ matrix in which the ratios can be stored. The columns represent the n tiles in the grid and the rows represent the m ultrasound lines between transmitters and sensors. This way the ratio in cell (a, b) represents the ratio of the b^{th} line that crosses the a^{th} tile. If we introduce vector **x** of length n containing the mean times of flight on each tile and vector **b** of length m containing the mean times of flight over each ultrasound line, then a linear equation can be formulated:

$$\mathbf{x} = \mathbf{b} \cdot A^{-1} \tag{6}$$

When all ratios are put into matrix A, the matrix becomes singular and thus can not be inverted. Arnold K. et al. [5] use the Simultaneous Iterative Reconstruction Technique (SIRT) to find a solution in a similar case. This technique uses the following equation:

$$\mathbf{x}(t+1) = \mathbf{x}(t) + CA^T R(\mathbf{b} - A\mathbf{x}(t)) \tag{7}$$

Where **x** is a guess for the mean temperatures on each tile, with initial guess **x**(0) = **0**. Matrices C and R are diagonal matrices containing respectively the sums of the columns and rows of matrix A. Together they give a weight factor for how many ultrasound rays cross each tile. Multiplied with the transposed version of A they form a correction that is multiplied by a factor. This factor depends on how big the difference is between the guess and the actual solution and is then added to **x**(t). This iterates until **x**(t) converges.

Another way to take the inverse of matrix A, is to use the Moore-Penrose pseudoinverse, used by M.M. Bronstein

et al. [6]. This pseudoinverse gives a least squares solution for the linear equation $A \cdot \mathbf{x} = \mathbf{b}$.

SIRT and the pseudoinverse give times of flight for each tile. The temperatures can be determined with formula 2.

The SIRT and pseudoinverse algorithms can both work with temperature or time of flight as input. To validate these two methods, a test algorithm was designed that uses mean temperatures over the ultrasound lines. With data from the sensor nodes, a temperature mapping was created using interpolation. This mapping was used to calculate mean temperatures over the 48 lines between ultrasound transmitters and sensors. These were stored in vector **b** which was used as input for the SIRT and pseudoinverse algorithms. The image these algorithms gave were compared to the initial image made according to the sensor nodes. This was done for setups with 16, 36, 49 and 64 tiles.

IV. Results

A. Determining one line average temperature

1) unheated: The experiment with a one 2.00 meter line segment with 25 measurements without heater resulted in a standard deviation of less than 2 μs per measurement for all three methods, as shown in table I. This causes a standard deviation in the calculated temperature per measurement of less than 0.2 °C for all methods. The absolute error of T_{avg} compared to the real temperature, 21.9 $\pm$ 0.5 °C, as described in III-C, is less than 1.2 °C.

TABLE I
TIMES OF FLIGHT AND CALCULATED TEMPERATURE OF 25 MEASUREMENTS WITHOUT HEATER

method nr.	ToF_{avg} [ms]	σ_t [ms]	T_{avg} [°C]	σ_T [°C]
1	5.8134	0.0008	21.31	0.08
2	5.8024	0.0014	22.51	0.15
3	5.8063	0.0013	22.12	0.13

2) heated: The experiment with heater resulted in a higher standard deviation in time of flight. The highest standard deviation, as shown in table II is 6 μs. Table II displays the T_{avg} that follow from the times of flight. The standard deviations increase to 0.4-0.6 °C. The absolute error lies between 0 and 2 °C.

TABLE II
TIMES OF FLIGHT AND CALCULATED TEMPERATURE OF 25 MEASUREMENTS WITH HEATER

method nr.	ToF_{avg} [ms]	σ_t [ms]	T_{avg} [°C]	σ_T [°C]
1	5.772	0.006	25.6	0.6
2	5.768	0.005	26.0	0.5
3	5.769	0.004	25.9	0.4

From these results it follows that it is possible to determine temperature in the circumstances as described in section III-C, within the above-mentioned error margins, using ultrasound time of flight.

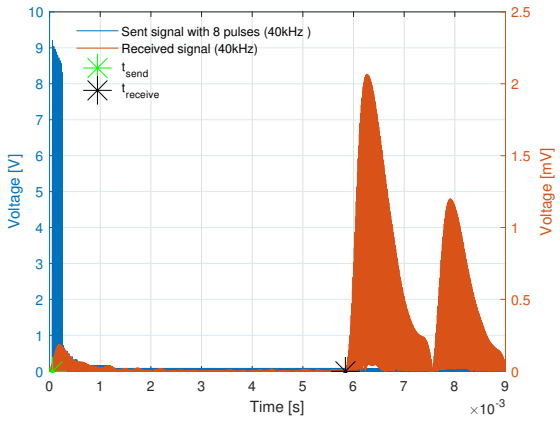

Fig. 3. Absolute values of sending and receiving signal of the ultrasound transducer for one measurement

B. SIRT and pseudoinverse

The results of the comparisons of mapping with the SIRT and pseudoinverse algorithms to the sensor node mapping are presented in table III. This table gives the average, minimum and maximum deviation of the temperatures that the SIRT and pseudoinverse algorithms have compared to the temperatures the sensor nodes give for each tile. When mapping over less tiles than there are ultrasound lines, which is the case with 16 and 36 tiles, both algorithms have a deviation so close to zero that it is much smaller than the fault made when measuring the time of flight. Mapping over 49 and 64 tiles means having more tiles than ultrasound lines. In these situations the SIRT algorithm is able to reconstruct almost the same picture as the sensor nodes do, whereas the pseudoinverse has much larger deviations. Figure 4 shows an example of a spatial temperature mapping by SIRT.

TABLE III
DEVIATION OF SIRT COMPARED TO SENSOR NODES

Tiles	Algorithm	$\sigma_{average}$ [°C]	σ_{min} [°C]	σ_{max} [°C]
49	SIRT	0.16	0.0	0.59
	pinv	0.63	0.0	2.8
64	SIRT	0.98	0.0	3.1
	pinv	2.6	0.0	13

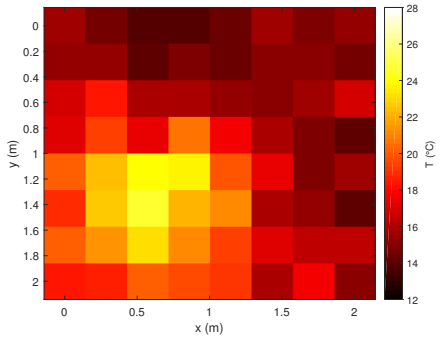

Fig. 4. Example of an 8x8 tiles temperature mapping using SIRT

V. Discussion

A. Temperature mapping using time of flight

The experiment has shown that it is possible to determine temperature using time of flight. However, the used hardware did not allow for measuring all line averages within a reasonable amount of time in which the temperature distribution could be considered to be constant. Also, determining all line averages would include lines that are too small for a sufficient precision due to the errors explained in section V-B.

B. Error analysis

Using a tape measure, and estimating the exact place of the piezo, leads to a total systematical error of the distance up to $\pm$ 4.5 mm. This causes a systematical temperature error of up to $\pm$ 1.5 °C at a distance of 2.00 meters. The absolute error of the distance stays the same for smaller distances , causing larger errors in temperature. Equation 2 assumes dry air, whilst humidity has an effect on the speed of sound of up to 0.5 % at 25 °C [7].This error is systematical within a time span in which humidity stays constant.

Using methods 1-3 for determining $t_{receive}$ may result in significant random errors. The main reason is that the signal to noise ratio is low, often less than one, around $t_{receive}$ as shown in figure 5. The root-mean-square value of the 40 kHz noise of the receiver is around 4-7 μV which is too high for consistently determining $t_{receive}$ very accurately. A miscalculation in determining $t_{receive}$ of half a 40 kHz cycle leads to a difference in temperature calculation of at least 1 °C at 2.00 meters, or more for smaller distances.

Air flow causes the received signal to become weaker. The air flow due to the heater causes a voltage decline of almost a factor 3 when the signal arrives.

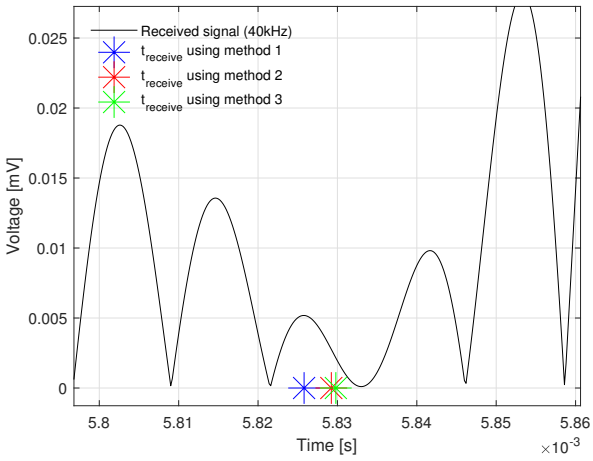

Fig. 5. Absolute values of sent and received signal of the ultrasound transducer for one measurement, zoomed in on $t_{receive}$.

VI. Conclusions

A. Conclusions

Using time of flight measurements, it is possible to determine temperature. However, determining temperature with the same precision as using a conventional method such as sensor nodes, requires a very high precision in determining time of flight. This is due to small errors having large effects on temperature calculation. Early research, [1] [2] [3], only showed a shallow substantiation of the algorithms used. In this research times of flight of ultrasound lines over a field are used as input, the SIRT or pseudoinverse algorithms can be used to retrieve a spatial temperature mapping. This is done without in-field measurements. In contrary, when using sensor nodes, a spatial temperature mapping is only possible with in-field sensors. This research combined a larger field than [2] and [3] with ultrasound instead of 1000 Hz [1].

B. Recommendations

The determination of the start of the signal can be optimized. The method described by Sarabia et al. [8] might provide a more precise $t_{receive}$ and thus a more accurate temperature estimation.

Measuring each line in the test grid by hand takes approximately one hour. A much more thorough hardware and software based solution is required to do testing in a shorter time span, in which temperature is constant. Multiple receivers might be read at once as long as $t_{receive}$ of each received signal can be distinguished.

The shortest lines in this setup lead to a precision that is too low when measuring time of flight, so it is advisable to first investigate the minimal distance over which time of flight can be measured accurately, before building a setup.

Acknowledgements

A special thanks goes to our supervisors P.G. Steeneken and G.J. Verbiest for guiding us through our research.

References

[1] A. Raabe, K. Arnold, and A. Ziemann, "Near surface spatially averaged air temperature and wind speed determined by acoustic travel time tomography," *Meteorologische Zeitschrift*, vol. 10, no. 1, pp. 61–70, 2001.

[2] K. Mizutani, K. Nishizaki, K. Nagai, and K. Harakawa, "Measurement of temperature distribution in space using ultrasound computerized tomography," *Japanese journal of applied physics*, vol. 36, no. 5S, p. 3176, 1997.

[3] S. Ohyama, J. Takayama, Y. Watanabe, T. Takahoshi, and K. Oshima, "Temperature distribution and wind vector measurement using ultrasonic ct based on the time of flight detection," *Sensors and Actuators A: Physical*, vol. 151, no. 2, pp. 159–167, 2009.

[4] F. Aldawi, A. P. Longstaff, S. Fletcher, P. Mather, and A. Myers, "A high accuracy ultrasound distance measurement system using binary frequency shift-keyed signal and phase detection." University of Huddersfield, 2007.

[5] K. Arnold, A. Ziemann, and A. Raabe, "Acoustic tomography inside the atmospheric boundary layer," *Physics and Chemistry of the Earth, Part B: Hydrology, Oceans and Atmosphere*, vol. 24, no. 1-2, pp. 133–137, 1999.

[6] M. M. Bronstein, A. M. Bronstein, M. Zibulevsky, and H. Azhari, "Reconstruction in diffraction ultrasound tomography using nonuniform fft," *IEEE transactions on medical imaging*, vol. 21, no. 11, pp. 1395–1401, 2002.

[7] G. S. Wong and T. F. Embleton, "Variation of the speed of sound in air with humidity and temperature," *The Journal of the Acoustical Society of America*, vol. 77, no. 5, pp. 1710–1712, 1985.

[8] E. Sarabia, J. Llata, S. Robla, C. Torre-Ferrero, and J. Oria, "Accurate estimation of airborne ultrasonic time-of-flight for overlapping echoes," *Sensors*, vol. 13, no. 11, pp. 15 465–15 488, 2013.